Impact of Personal Characteristics and Technical Factors on Quantification of Sodium ^{18}F-Fluoride Uptake in Human Arteries: Prospective Evaluation of Healthy Subjects

Björn Alexander Blomberg[1,2], Anders Thomassen[1], Pim A. de Jong[2], Jane A. Simonsen[1], Marnix G.E.H. Lam[2], Anne L. Nielsen[1], Hans Mickley[3], Willem P.T.M. Mali[2], Abass Alavi[4], and Poul F. Høilund-Carlsen[1,5]

[1]Department of Nuclear Medicine, Odense University Hospital, Odense, Denmark; [2]Department of Radiology and Nuclear Medicine, University Medical Center Utrecht, Utrecht, The Netherlands; [3]Department of Cardiology, Odense University Hospital, Odense, Denmark; [4]Department of Radiology, Hospital of the University of Pennsylvania, Philadelphia, Pennsylvania; and [5]Institute of Clinical Research, University of Southern Denmark, Odense, Denmark

Sodium ^{18}F-fluoride (^{18}F-NaF) PET/CT imaging is a promising imaging technique for the assessment of atherosclerosis but is hampered by a lack of validated quantification protocols. Both personal characteristics and technical factors can affect quantification of arterial ^{18}F-NaF uptake. This study investigated whether blood activity, renal function, injected dose, circulating time, and PET/CT system affect quantification of arterial ^{18}F-NaF uptake. **Methods:** Eighty-nine healthy subjects were prospectively examined by ^{18}F-NaF PET/CT imaging. Arterial ^{18}F-NaF uptake was quantified at the level of the ascending aorta, aortic arch, descending thoracic aorta, and coronary arteries by calculating the maximum ^{18}F-NaF activity (NaFmax), the maximum/mean target-to-background ratio (TBRmax/mean), and the maximum blood-subtracted ^{18}F-NaF activity (bsNaFmax). Multivariable linear regression assessed the effect of personal characteristics and technical factors on quantification of arterial ^{18}F-NaF uptake. **Results:** NaFmax and TBRmax/mean were dependent on blood activity (β = 0.34 to 0.44, $P < 0.001$, and β = −0.68 to −0.58, $P < 0.001$, respectively) and PET/CT system (β = −0.80 to −0.53, $P < 0.001$, and β = −0.80 to −0.23, $P < 0.031$, respectively). bsNaFmax depended on PET/CT system (β = −0.91 to −0.57, $P < 0.001$) but not blood activity. This finding was observed at the level of the ascending aorta, aortic arch, descending thoracic aorta, and the coronary arteries. In addition to blood activity and PET/CT system, injected dose affected quantification of arterial ^{18}F-NaF uptake, whereas renal function and circulating time did not. **Conclusion:** The prospective evaluation of 89 healthy subjects demonstrated that quantification of arterial ^{18}F-NaF uptake is affected by blood activity, injected dose, and PET/CT system. Therefore, blood activity, injected dose, and PET/CT system should be considered to generate accurate estimates of arterial ^{18}F-NaF uptake.

Key Words: PET/CT; sodium ^{18}F-fluoride (^{18}F-NaF); atherosclerosis; vascular calcification; quantification

Sodium ^{18}F-fluoride (^{18}F-NaF) PET/CT is a promising noninvasive imaging technique for the assessment of atherosclerosis. ^{18}F-NaF PET/CT targets the active exchange of fluoride with hydroxyl ions of hydroxylapatite crystals producing fluorapatite (1). This process is believed to represent calcification metabolism of osseous tissue, including vascular calcification (2–4). By imaging vascular calcification metabolism, ^{18}F-NaF PET/CT can potentially identify patients at high cardiovascular risk (4) and improve cardiovascular risk stratification (5,6).

Although ^{18}F-NaF PET/CT imaging of vascular calcification is promising, the implementation of ^{18}F-NaF PET/CT in research and clinical settings is hampered by a lack of validated and standardized quantification protocols. Most studies quantify arterial ^{18}F-NaF uptake as the ratio between arterial wall and blood ^{18}F-NaF activity, known as the maximum/mean target-to-background ratio (TBRmax/mean). However, this method has been criticized as being too dependent on blood activity (6). In addition to blood activity, quantification of arterial ^{18}F-NaF uptake can be affected by personal characteristics and technical factors, including body weight, body surface area, renal function, injected ^{18}F-NaF dose, ^{18}F-NaF circulating time, and PET/CT system. It is not known which factors affect quantification of arterial ^{18}F-NaF uptake. Standardized and unbiased quantification of arterial ^{18}F-NaF uptake is imperative for both research and clinical settings, being a prerequisite for generation of reference values for arterial ^{18}F-NaF uptake with healthy aging, for response evaluation requiring repeated ^{18}F-NaF PET/CT examinations, and to allow for comparison of quantitative imaging results among studies.

The purpose of this study was to determine the effect of personal characteristics and technical factors on the quantification of arterial ^{18}F-NaF uptake. By studying these effects in a group of healthy subjects, we aimed to generate accurate estimates of arterial ^{18}F-NaF uptake. Secondary aims were to elucidate the effects of quantification methods on estimates of arterial ^{18}F-NaF uptake, to determine the optimal location for assessment of blood activity, and finally, to evaluate rater reliability and agreement.

MATERIALS AND METHODS

This study is part of the Cardiovascular Molecular Calcification Assessed by ^{18}F-NaF PET/CT (CAMONA) study. CAMONA was approved by the Danish National Committee on Health Research Ethics,

registered at ClinicalTrials.gov (NCT01724749), and conducted in accordance with the Declaration of Helsinki. Written informed consent was obtained from all study subjects.

Subject Selection

Healthy subjects were prospectively recruited from the general population by local advertisement or from the blood bank of Odense University Hospital, Denmark. Subjects free of oncologic disease, autoimmune disease, immunodeficiency syndromes, alcohol abuse, illicit drug use, (symptoms suggesting) cardiovascular disease, or prescription medication were considered healthy and were eligible for inclusion. Pregnant women were not considered for inclusion. Healthy subjects were recruited to limit bias from cardiovascular disease on study results. Subjects were preselected by sex and age to secure a balanced inclusion of men and women aged 20–29, 30–39, 40–49, 50–59, and older than 60 y. This selection process allowed us to study a wide range of subjects to ensure translation of our findings to various settings.

Study Design

Healthy subjects were evaluated by blood pressure measurements, blood analyses, ^{18}F-NaF PET/CT imaging, and unenhanced cardiac CT imaging. Blood pressure measurements were performed 3 times after a supine rest of at least 30 min. The average of the last 2 measurements determined the systolic and diastolic blood pressure. Blood analyses included fasting serum total cholesterol, serum low-density lipoprotein cholesterol, serum high-density lipoprotein cholesterol, serum triglycerides, fasting plasma glucose, glycated hemoglobin (HbA1c), and serum creatinine, with serum creatinine being used to calculate the Modification of Diet and Renal Disease (MDRD) estimated glomerular filtration rate (eGFR). Furthermore, body weight, body height, body mass index, and body surface area according to Du Bois were determined. ^{18}F-NaF PET/CT imaging was performed on integrated PET/CT systems (Discovery 690/710, STE, VCT, and RX; GE Healthcare) at the PET center of Odense University Hospital, Denmark. Subjects were allocated to a PET/CT system at the discretion of the department's booking system. PET/CT system specifications and image reconstruction parameters are summarized in Supplemental Table 1 (supplemental materials are available at http://jnm.snmjournals. org). Each subject underwent PET/CT imaging at approximately 90 min after intravenous injection of approximately 2.2 MBq of ^{18}F-NaF per kilogram of body weight (6). The emission acquisition duration per bed position was 2.5 min. Total-body PET images were acquired in 3-dimensional mode and reconstructed into coronal, axial, and sagittal planes by an ordered-subsets expectation maximization algorithm (VUE Point; GE Healthcare). PET images were corrected for attenuation, scatter, random coincidences, and scanner dead time. Low-dose CT imaging (140 kV; 30–110 mA; noise index, 25; 0.8 s per rotation; slice thickness, 3.75 mm) was performed for attenuation correction and anatomic orientation. To determine the coronary calcium score, unenhanced, breath-hold, cardiac CT imaging (120 kV; 100 mA; 0.4 s per rotation; slice thickness, 2.5 mm) was performed with electrocardiogram gating at 50% of the R-R interval. The effective radiation dose received for the entire imaging protocol was approximately 11 mSv.

Quantitative Image Analyses

All images were analyzed using the IntelliSpace Portal client (version 4.0; Philips Healthcare). The image analyst was masked to subject demographics and PET/CT system specifications. For each subject, uptake of ^{18}F-NaF was determined in the ascending aorta, aortic arch, descending thoracic aorta, and coronary arteries according to previously published methods (6). In summary, for the coronary arteries, we manually drew a free-hand region of interest (ROI) around the cardiac silhouette on every slice of the axially oriented PET/CT images. We carefully excluded ^{18}F-NaF activity originating from bone tissue and cardiac valves by eliminating these areas from the ROI. For the aorta, we manually drew a free-hand ROI around the outer perimeter of the artery on every slice of the axially oriented PET/CT images. We carefully excluded skeletal-derived ^{18}F-NaF activity by eliminating these areas from the ROI. Per ROI, the maximum radiotracer-decay-corrected ^{18}F-NaF activity (kBq/mL) was determined. Per arterial bed, maximum values obtained per ROI were summed and divided by the number of ROIs resulting in a single averaged maximum value (NaFmax) for the ascending aorta, aortic arch, descending thoracic aorta, and coronary arteries. Blood ^{18}F-NaF activity was determined in the lumen of the right atrium, aortic arch, right and left internal jugular veins, superior and inferior vena cava, and right and left femoral veins. Blood ^{18}F-NaF activity was determined by drawing a single ROI in the center of each vessel (or atrium) and was quantified as the radiotracer-decay-corrected mean ^{18}F-NaF activity (bloodNaFmean). Quantification of blood ^{18}F-NaF activity is summarized in Supplemental Figure 1. To correct for blood ^{18}F-NaF activity, NaFmax was divided and subtracted by bloodNaFmean, respectively, to generate the TBRmax/mean and maximum blood-subtracted ^{18}F-NaF activity (bsNaFmax). Blood-pool correction was performed with superior vena cava bloodNaFmean only, because this location was least subject to spillover activity from adjacent ^{18}F-NaF–avid structures. In addition, super vena cava bloodNaFmean could be determined with excellent inter- and intrarater agreement (Supplemental Tables 2 and 3). The quantification of arterial ^{18}F-NaF uptake is summarized in Figure 1. The coronary calcium score, obtained from the cardiac CT images, was quantified in arbitrary units according to Agatston and as a volumetric score (mm^3) (7).

Rater Reliability and Agreement

Inter- and intrarater reliability and agreement of NaFmax and bloodNaFmean were assessed 2 mo after the initial analysis in a
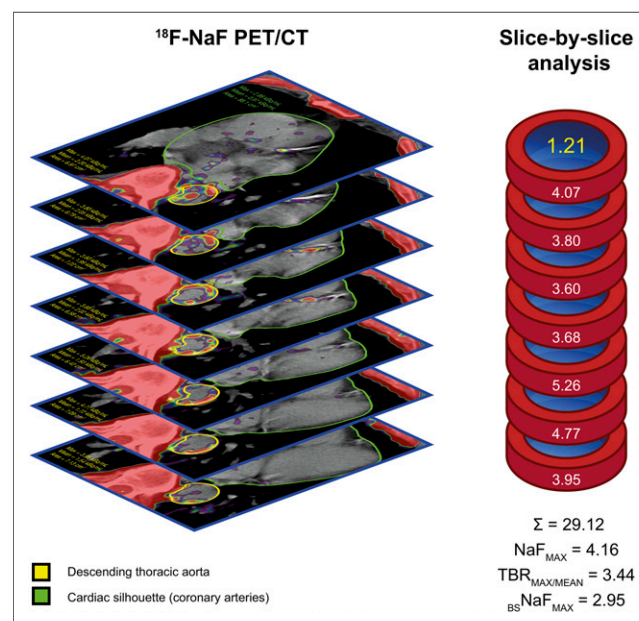

FIGURE 1. Illustration demonstrating quantification of arterial ^{18}F-NaF uptake. ROI is drawn around arterial wall (yellow ROI = descending thoracic aorta) or cardiac silhouette (green ROI) on every slice of axially oriented ^{18}F-NaF PET/CT images. Per ROI, maximum ^{18}F-NaF activity is determined. Values obtained per ROI are summed (Σ) and averaged (NaFmax) and subsequently divided or subtracted by mean ^{18}F-NaF blood activity (bloodNaFmean). This process provides TBRmax/mean or blood-subtracted ^{18}F-NaF activity (bsNaFmax), respectively. bloodNaFmean was estimated in superior vena cava (not shown).

TABLE 1
Subject Demographics

Demographic	Total (n = 89)	Minimum	Maximum
Age (y)	44 ± 14	21	75
Male (n)	47 (53)		
Active smoking (n)	3 (3)		
Blood pressure (mm Hg)			
Systolic	128 ± 17	98	201
Diastolic	77 ± 10	57	107
Body weight (kg)	80.2 ± 18.3	49.8	145.4
Body surface area (m^2)	1.93 ± 0.24	1.54	2.67
Body mass index (kg/m^2)	26.6 ± 4.4	17.6	42.5
Cholesterol (mmol/L)			
Total	4.9 ± 0.9	2.9	7.4
Low-density lipoprotein	3.1 ± 0.8	1.3	5.0
High-density lipoprotein	1.4 ± 0.5	0.7	3.2
Triglycerides (mmol/L)	1.0 ± 0.7	0.3	4.5
Plasma glucose (mmol/L)	5.5 ± 0.5	4.4	6.7
HbA1c (mmol/mol)	33.9 ± 4.1	24.0	49.0
Creatinine (μmol/L)	79.3 ± 13.1	52.0	118.0
MDRD-eGFR (mL/min/1.73 m^2)	82.9 ± 13.2	55.0	113.0
Coronary calcium score			
Agatston score (arbitrary units)	0 [0 and 0]	0	1,046
Volume (mm^3)	0 [0 and 0]	0	430
Injected dose (MBq)	174 ± 39	109	348
Circulation time (min)	92 ± 4	90	109
NaFmax (kBq/mL)			
Ascending aorta	3.32 ± 1.17	1.69	6.43
Aortic arch	3.25 ± 1.07	1.36	7.16
Descending aorta	3.22 ± 0.88	1.64	5.92
Coronary arteries	3.75 ± 0.91	2.03	6.13
PET/CT system (n)			
Discovery STE	22 (25)		
Discovery VCT	19 (21)		
Discovery RX	28 (31)		
Discovery 690/710	20 (22)		

Values are mean ± SD; n, with percentages in parentheses; or median, with 25 and 75 percentiles in brackets for 89 subjects.

randomly selected sample of 10 subjects. Raters were masked for subject demographics, imaging specifications, and results from the initial analysis.

Statistical Analysis

Subject demographics were summarized by descriptive statistics. Mean bloodNaFmean was compared among vascular beds by the repeated measures 1-way ANOVA. Multivariable linear regression assessed the dependence of bloodNaFmean, NaFmax, TBRmax/mean, and bsNaFmax on personal characteristics and technical factors. We did not evaluate nonlinear or interaction effects. First, we tested whether the assumptions of no multicollinearity (tolerance statistic), independent errors (Durbin–Watson statistic), and homoscedasticity (graphically) between predictor variables were met. The assumption of no multicollinearity was violated by our predictor variables. Multicollinearity existed between injected dose, body weight, and body surface area (Supplemental Fig. 2). The issue of multicollinearity was resolved by removing body weight and body surface area from the regression analyses. Subsequently, stepwise selection of variables, based on Akaike information criterion, was performed by a backward elimination strategy. The categoric variable PET/CT system was entered as a factor into the model with the Discovery 690/710 as a reference system. Variables not selected by the model were considered not related to arterial ^{18}F-NaF uptake. Variability in variable selection was evaluated and adjusted for by a bootstrap of 2,000 samples (8). Rater reliability was assessed by the intraclass correlation coefficient (2-way random-effects model assessing absolute agreement of single measures) (9). Rater agreement was assessed by calculation of the

95% limits of agreement according to Bland and Altman (*10*). A 2-tailed *P* value below 0.05 was regarded statistically significant. To internally validate our results, *P* values and 95% confidence intervals were determined by a bootstrap of 2,000 samples. The sample size was based on the regression analysis. For every predictor variable (i.e., 6 continuous and 1 categoric variable), we aimed to include 10 subjects, resulting in a sample size of 90 subjects. Statistical analyses were performed by statistical software R (version 3.1.2; The R Foundation for Statistical Computing), combined with the packages bootStepAIC, version 1.2-0; MASS, version 7.3-35; car, version 2.0-22; and QuantPsyc, version 1.5.

RESULTS

Between November 2012 and May 2014, we prospectively recruited 90 healthy subjects. One subject was excluded from the analysis because she refused the PET/CT examination due to claustrophobia. Subject demographics are summarized in Table 1.

bloodNaFmean was significantly different among vessel beds ($F_{7,704} = 66.6$; $P < 0.001$) (Fig. 2). In particular, left internal jugular vein bloodNaFmean was up to 58% higher than bloodNaFmean in other vascular beds ($t = 10.2$; $P < 0.001$). Similarly, right internal jugular vein bloodNaFmean was up to 39% higher than bloodNaFmean in other vascular beds ($t = 12.0$; $P < 0.001$). Smaller, yet statistically significant, differences were observed between bloodNaFmean in the right atrium, aortic arch, superior vena cava, inferior vena cava, and femoral veins. Subsequent analyses were performed with superior vena cava bloodNaFmean only, because superior vena cava bloodNaFmean was least subject to spillover activity from adjacent ^{18}F-NaF–avid structures and demonstrated excellent rater agreement (Fig. 2; Supplemental Tables 2 and 3). Superior vena cava bloodNaFmean significantly depended on injected dose and PET/CT system (Table 2). For every 100-MBq increase in injected dose, bloodNaFmean increased

FIGURE 2. Box plots of mean ^{18}F-NaF blood activity (bloodNaFmean) estimated in various vascular beds at 90 min after injection of ^{18}F-NaF. Blood activity in right and left internal jugular veins was significantly higher ($P < 0.001$) than in other vascular beds. Activity in aortic arch was significantly higher than in superior vena cava ($P < 0.001$), inferior vena cava ($P = 0.017$), and right femoral vein ($P = 0.001$). bloodNaFmean was significantly lower in superior vena cava than in right atrium ($P < 0.001$) and inferior vena cava ($P = 0.010$). Filled circles represent outliers. Significance based on repeated-measures ANOVA with Bonferroni adjustment.

by 0.35 kBq/mL. bloodNaFmean was significantly higher among subjects examined using the Discovery 690/710 scanner than subjects examined using the Discovery VCT scanner. Superior vena cava bloodNaFmean did not depend on variations in renal function or circulating time.

At all levels of the arterial tree, NaFmax was significantly affected by blood activity and PET/CT system. For every kBq/mL increase in bloodNaFmean, NaFmax increased by 0.92–0.97 kBq/mL for the aorta and by 0.86 kBq/mL for the coronary arteries. NaFmax was significantly higher among subjects examined using the Discovery 690/710 scanner than subjects examined using the Discovery STE, VCT, or RX scanner. In addition to blood activity and PET/CT system, descending thoracic aortic NaFmax was significantly affected by renal function ($\beta = -0.15$, $P = 0.014$), and ascending aorta NaFmax was significantly affected by renal function ($\beta = -0.11$, $P = 0.020$) and injected dose ($\beta = 0.19$, $P = 0.008$). NaFmax was not affected by variations in circulating time (Table 3; Supplemental Tables 4–6).

At all levels of the arterial tree, TBRmax/mean was significantly affected by blood activity and PET/CT system. For every kBq/mL increase in bloodNaFmean, TBRmax/mean decreased by 1.15–1.27 for the aorta and 1.63 for the coronary arteries. TBRmax/mean was significantly higher among subjects examined using the Discovery 690/710 scanner than subjects examined using the Discovery STE, VCT, or RX scanners. In addition to blood activity and PET/CT system, coronary TBRmax/mean was significantly affected by injected dose ($\beta = 0.30$, $P = 0.020$), and ascending aorta TBRmax/mean was significantly affected by injected dose ($\beta = 0.33$, $P = 0.001$) and renal function ($\beta = -0.12$, $P = 0.034$). TBRmax/mean was not affected by variations in circulating time (Table 3; Supplemental Tables 4–6).

At all levels of the arterial tree, bsNaFmax was significantly affected by PET/CT system. bsNaFmax was significantly higher among subjects examined using the Discovery 690/710 scanner than subjects examined using the Discovery STE, VCT, or RX scanners. In addition to PET/CT system, descending thoracic aorta bsNaFmax was significantly affected by renal function ($\beta = -0.18$, $P = 0.016$), and ascending aorta bsNaFmax was significantly affected by renal function ($\beta = -0.13$, $P = 0.019$) and injected dose ($\beta = 0.21$, $P = 0.006$). bsNaFmax was not affected by variations in blood activity or circulating time (Table 3; Supplemental Tables 4–6).

DISCUSSION

Prospective evaluation of 89 healthy subjects demonstrated that quantification of arterial ^{18}F-NaF uptake is significantly affected by blood ^{18}F-NaF activity, ^{18}F-NaF injected dose, and PET/CT system but not renal function and ^{18}F-NaF circulating time. Therefore, blood activity, injected dose, and PET/CT system should be considered to generate unbiased estimates of arterial ^{18}F-NaF uptake.

To account for blood activity, it has been proposed to calculate the ratio between arterial wall ^{18}F-NaF uptake and blood ^{18}F-NaF activity, known as the TBRmax/mean (*3,5*). However, the TBRmax/mean has been criticized as being too dependent on variations in blood activity (*6*). Our study confirmed that TBRmax/mean is dependent on variations in blood activity. Therefore, quantifying arterial ^{18}F-NaF uptake as TBRmax/mean may result in biased estimates of arterial ^{18}F-NaF uptake. In contrast, our study demonstrated that bsNaFmax does not depend on blood activity. Therefore, we prefer to quantify arterial ^{18}F-NaF uptake as bsNaFmax over TBRmax/mean. Our preference cannot be substantiated by our data alone.
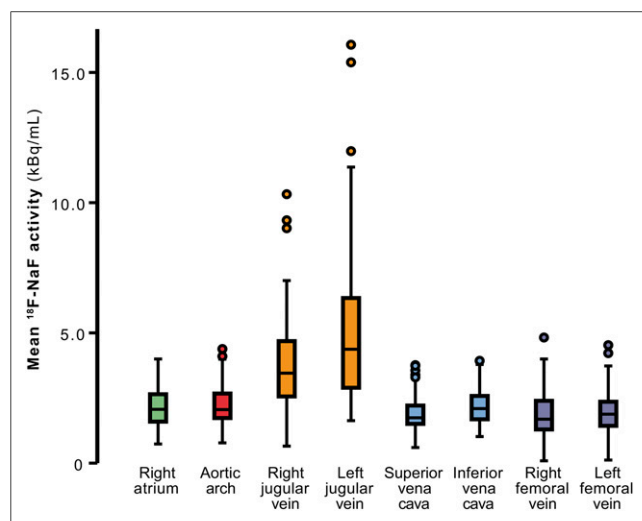
TABLE 2
Determinants of Mean ¹⁸F-NaF Blood Activity in Vena Cava Superior

Determinant	Regression coefficient	β	Adjusted R^2	P
bloodNaFmean (kBq/mL)			0.23	<0.001
Intercept (kBq/mL)	0.84 (0.42–1.49)			0.001
Injected dose (100 MBq)	0.35 (0.03–0.55)	0.32		0.011
PET/CT system				
Discovery STE	−0.14 (−0.36 to 0.13)	−0.14		0.310
Discovery VCT	−0.39 (−0.61 to −0.16)	−0.37		<0.001
Discovery RX	−0.01 (−0.23 to 0.19)	−0.01		0.948

β = standardized regression coefficient.
Model eliminated renal function and circulating time. 95% confidence intervals are presented in parentheses.

For that, autoradiographic and histologic analyses of arterial ¹⁸F-NaF uptake are necessary.

In studies that investigate vascular calcification metabolism with ¹⁸F-NaF PET/CT, blood activity is commonly estimated in the superior vena cava, inferior vena cava, or right atrium (3–6,11–14). However, it is not known whether estimates of blood activity are comparable among vessel beds. Theoretically, blood activity should be similar in intensity throughout the body, especially after prolonged circulating times. Nonetheless, our study demonstrated that estimates of blood activity differ significantly among vascular beds. In particular, recorded blood activity was higher in the right and left internal jugular veins than in other vascular beds. Spillover activity from adjacent ¹⁸F-NaF–avid structures likely accounts for this observation. For example, we believe that spillover activity from the skeleton, including the sternum, clavicles, and cervical spine, increases blood ¹⁸F-NaF activity estimates in the internal jugular veins. Similarly, we speculate that spillover activity from vascular calcifications may increase blood ¹⁸F-NaF activity estimates in the aortic arch. Therefore, we advise fixing the location of blood ¹⁸F-NaF activity estimation to the lumen of the superior vena cava, because this location is easy to identify and is largely devoid of spillover activity from adjacent ¹⁸F-NaF–avid structures. In addition, our study demonstrated that blood ¹⁸F-NaF activity could be determined with higher inter- and intrarater agreement at this location. The excellent rater agreement suggests that blood activity can be accurately estimated via placement of a single ROI as compared with multiple ROIs over several slices as propagated by some authors (13). In summary, standardized estimation of blood activity may reduce systematic errors and increase interstudy comparability.

In addition to blood activity, renal function affected the quantification of arterial ¹⁸F-NaF uptake. Renal function, expressed as MDRD-eGFR, negatively associated with NaFmax, TBRmax/mean, and bsNaFmax. Theoretically, impaired renal function prolongs tracer availability and may contribute to increased ¹⁸F-NaF accumulation in vascular calcifications. However, our study demonstrated that blood ¹⁸F-NaF activity did not depend on variations in MDRD-eGFR. Therefore, it seems unlikely that impaired renal function influences quantification of arterial ¹⁸F-NaF uptake by prolonging tracer availability. We believe that impaired renal function is a risk factor for the development of vascular calcification and consequently drives the degree of arterial ¹⁸F-NaF uptake, instead of affecting its quantification. This view finds support in studies that demonstrated strong positive associations between impaired renal function and increased prevalence of vascular calcifications (15–17). We acknowledge, however, that the impact of renal function on quantification of arterial Na¹⁸F uptake was studied in a healthy population. Therefore, it remains to be determined whether our findings can be replicated in a more diseased population, such as in patients with severe renal insufficiency.

In addition to blood activity and renal function, injected ¹⁸F-NaF dose affected quantification of arterial ¹⁸F-NaF uptake. The impact of injected ¹⁸F-NaF dose is related to the distribution volume of ¹⁸F-NaF. An increase in body size, and hence distribution volume, may negatively impact the uptake of ¹⁸F-NaF in the target organ, such as the arterial wall. To overcome this problem, our study administered an ¹⁸F-NaF dosage proportional to the subject's body weight. However, our regression models demonstrated that arterial ¹⁸F-NaF uptake increased linearly to injected dose for arterial segments, suggesting overcompensation for the negative impact of distribution volume on arterial ¹⁸F-NaF uptake. Calculation of the standardized uptake value (SUV) may account for variations in injected dose and distribution volume of ¹⁸F-NaF. The SUV is the decay-corrected activity concentration of ¹⁸F-NaF (kBq/mL) adjusted for injected dose (MBq) and body surface area (cm²) or body weight (kg). However, the observed multicollinearity between injected dose, body weight, and body surface area prevented SUV from adequately correcting for variations in injected dose and distribution volume of the tracer (Supplemental Fig. 3). To overcome issues surrounding injected ¹⁸F-NaF dose, we advise administration of a fixed ¹⁸F-NaF dose in studies evaluating vascular calcification with ¹⁸F-NaF PET/CT and taking the effect of distribution volume of the tracer separately into account.

In addition to blood activity, renal function, and injected dose, quantification of arterial ¹⁸F-NaF uptake was affected by differences in PET/CT technology. Even though our imaging protocol adhered to international practice guidelines (18) and our PET/CT systems were calibrated to a phantom, subjects examined using the Discovery 690/710 scanner had significantly higher arterial ¹⁸F-NaF uptake than subjects examined on our older PET/CT systems (i.e., Discovery STE, VCT, or RX scanners). Differences in imaging hardware and software likely account for this observation (Supplemental Table 1). It remains challenging to cross-calibrate PET/CT systems to overcome differences in imaging hardware and software, even if PET/CT systems are from the same vendor, as was the case in our study. Our study considered only PET/CT instrumentation from GE Healthcare that differed in generation.

TABLE 3
Determinants of ^{18}F-NaF Uptake in Ascending Aorta

Determinant	Regression coefficient	β	Adjusted R^2	P
NaFmax (kBq/mL)			0.80	<0.001
Intercept (kBq/mL)	3.54 (2.59 to 4.23)			<0.001
Blood activity (kBq/mL)	0.94 (0.65 to 1.21)	0.34		<0.001
MDRD-eGFR (mL/min/1.73 m^2)	−0.01 (−0.02 to −0.00)	−0.11		0.020
Injected dose (100 MBq)	0.57 (0.18 to 1.23)	0.19		0.008
PET/CT system				
Discovery STE	−2.16 (−2.56 to −1.76)	−0.80		<0.001
Discovery VCT	−2.14 (−2.55 to −1.74)	−0.75		<0.001
Discovery RX	−1.99 (−2.37 to −1.61)	−0.79		<0.001
TBRmax/mean			0.69	<0.001
Intercept	4.89 (4.03 to 5.68)			<0.001
Blood activity (kBq/mL)	−1.27 (−1.75 to −0.90)	−0.60		<0.001
MDRD-eGFR (mL/min/1.73 m^2)	−0.01 (−0.02 to −0.00)	−0.12		0.034
Injected dose (100 MBq)	0.77 (0.39 to 1.34)	0.33		0.001
PET/CT system				
Discovery STE	−1.67 (−2.03 to −1.33)	−0.80		<0001
Discovery VCT	−1.54 (−1.89 to −1.20)	−0.70		<0.001
Discovery RX	−1.55 (−1.86 to −1.24)	−0.80		<0.001
bsNaFmax (kBq/mL)			0.74	<0.001
Intercept (kBq/mL)	3.47 (2.63 to 4.10)			<0.001
MDRD-eGFR (mL/min/1.73 m^2)	−0.01 (−0.02 to −0.00)	−0.13		0.019
Injected dose (100 MBq)	0.55 (0.24 to 1.13)	0.21		0.006
PET/CT system				
Discovery STE	−2.15 (−2.52 to −1.78)	−0.91		<0.001
Discovery VCT	−2.12 (−2.49 to −1.78)	−0.86		<0.001
Discovery RX	−1.99 (−2.33 to −1.62)	−0.91		<0.001

β = standardized regression coefficient.

All models eliminated circulating time. In addition, blood activity was eliminated by model bsNaFmax. 95% confidence intervals are presented in parentheses.

Hence, we could not investigate the impact of PET/CT technology from different vendors on quantification of arterial ^{18}F-NaF. Therefore, we encourage additional research to determine whether differences in PET/CT technology are easier to overcome in systems that are similar in generation but differ in vendor. In addition, promising initiatives in ^{18}F-FDG PET/CT imaging, such as the EARL ^{18}F-FDG PET/CT accreditation program (19), may resolve issues surrounding differences in PET/CT technology and may contribute to improved interscan agreement in quantitative PET studies.

In contrast to blood activity, renal function, injected dose, and PET/CT system, ^{18}F-NaF-circulating time did not affect quantification of arterial ^{18}F-NaF uptake. In a previous study, our group demonstrated that circulating time affects quantification of arterial ^{18}F-NaF uptake (6). In 38 subjects imaged at 45, 90, and 180 min after ^{18}F-NaF administration, we demonstrated that the maximum SUV, a value related to NaFmax, and blood ^{18}F-NaF activity significantly decreased with time ($P < 0.001$ and <0.001, respectively), whereas the TBRmax/mean significantly increased with time ($P < 0.001$). The blood-subtracted maximum SUV, a value related to

bsNaFmax, was not affected by the circulating time ($P = 0.65$). In the present study, we fixed the circulating time of ^{18}F-NaF to approximately 90 min and demonstrated that quantification of arterial ^{18}F-NaF uptake was not affected by small variations in circulating time. Consequently, a fixed time between ^{18}F-NaF administration and PET/CT acquisition can adequately negate the impact of circulating time on quantification of arterial ^{18}F-NaF uptake.

Finally, our study demonstrated that quantification of arterial ^{18}F-NaF uptake and blood ^{18}F-NaF activity can be achieved with excellent inter- and intrarater reliability and agreement (Supplemental Tables 2 and 3). This finding is consistent with previous reports (5,6).

An important strength of the present study is that we prospectively evaluated the effect of personal characteristics and technical factors on arterial ^{18}F-NaF uptake in a group of healthy subjects. By studying healthy subjects, we limited bias from cardiovascular risk factors on the generated results. However, studying a healthy population prevents extrapolation of the results to a more diseased population. For example, only 6% of subjects had

impaired renal function (MDRD-eGFR $<$ 60 mL/min/1.73 m^2). Therefore, we remain cautious in extrapolating our results to subjects with severe renal insufficiency. Second, although our study results were internally validated by bootstrap techniques, they lack external validation. To overcome this limitation, our study should preferably be repeated in a different population by different researchers. Third, ethical considerations prevented collection of arterial specimens for histologic examination. Therefore, we could not associate arterial ^{18}F-NaF uptake to histologic markers of vascular calcification. For similar reasons, we could not collect invasive blood samples to determine and compare blood activity estimates obtained by PET/CT imaging to the true blood ^{18}F-NaF activity. Finally, the notion that quantification of arterial ^{18}F-NaF uptake by TBRmax/mean is suboptimal compared with bsNaFmax cannot be substantiated by our data alone. Comparing arterial ^{18}F-NaF uptake with autoradiographic and histologic analyses of vascular calcification may be able to confirm the notion that bsNaFmax is a preferred quantifier of arterial ^{18}F-NaF uptake.

CONCLUSION

Prospective evaluation of 89 healthy subjects demonstrated that quantification of arterial ^{18}F-NaF uptake is affected by blood ^{18}F-NaF activity, injected dose, and PET/CT system. These factors should be accounted for in quantification methodologies to generate accurate estimates of arterial ^{18}F-NaF uptake.

DISCLOSURE

ACKNOWLEDGMENTS

REFERENCES

1. Czernin J, Satyamurthy N, Schiepers C. Molecular mechanisms of bone ^{18}F-NaF deposition. *J Nucl Med.* 2010;51:1826–1829.
2. Derlin T, Richter U, Bannas P, et al. Feasibility of ^{18}F-sodium fluoride PET/CT for imaging of atherosclerotic plaque. *J Nucl Med.* 2010;51:862–865.
3. Derlin T, Wisotzki C, Richter U, et al. In vivo imaging of mineral deposition in carotid plaque using ^{18}F-sodium fluoride PET/CT: correlation with atherogenic risk factors. *J Nucl Med.* 2011;52:362–368.
4. Joshi NV, Vesey AT, Williams MC, et al. ^{18}F-fluoride positron emission tomography for identification of ruptured and high-risk coronary atherosclerotic plaques: a prospective clinical trial. *Lancet.* 2014;383:705–713.
5. Dweck MR, Chow MW, Joshi NV, et al. Coronary arterial ^{18}F-sodium fluoride uptake: a novel marker of plaque biology. *J Am Coll Cardiol.* 2012;59:1539–1548.
6. Blomberg BA, Thomassen A, Takx RA, et al. Delayed sodium ^{18}F-fluoride PET/CT imaging does not improve quantification of vascular calcification metabolism: results from the CAMONA study. *J Nucl Cardiol.* 2014;21:293–304.
7. Becker CR, Knez A, Ohnesorge B, et al. Visualization and quantification of coronary calcifications with electron beam and spiral computed tomography. *Eur Radiol.* 2000;10:629–635.
8. Austin PC, Tu JV. Bootstrap methods for developing predictive models. *Am Stat.* 2004;58:131–137.
9. Kottner J, Audige L, Brorson S, et al. Guidelines for Reporting Reliability and Agreement Studies (GRRAS) were proposed. *J Clin Epidemiol.* 2011;64:96–106.
10. Bland JM, Altman DG. Statistical methods for assessing agreement between two methods of clinical measurement. *Lancet.* 1986;1:307–310.
11. Derlin T, Janssen T, Salamon J, et al. Age-related differences in the activity of arterial mineral deposition and regional bone metabolism: a ^{18}F-sodium fluoride positron emission tomography study. *Osteoporos Int.* 2015;26:199–207.
12. Derlin T, Toth Z, Papp L, et al. Correlation of inflammation assessed by ^{18}F-FDG PET, active mineral deposition assessed by ^{18}F-fluoride PET, and vascular calcification in atherosclerotic plaque: a dual-tracer PET/CT study. *J Nucl Med.* 2011;52:1020–1027.
13. Janssen T, Bannas P, Herrmann J, et al. Association of linear ^{18}F-sodium fluoride accumulation in femoral arteries as a measure of diffuse calcification with cardiovascular risk factors: a PET/CT study. *J Nucl Cardiol.* 2013;20:569–577.
14. Morbelli S, Fiz F, Piccardo A, et al. Divergent determinants of ^{18}F-NaF uptake and visible calcium deposition in large arteries: relationship with Framingham risk score. *Int J Cardiovasc Imaging.* 2014;30:439–447.
15. Demer LL, Tintut Y. Vascular calcification: pathobiology of a multifaceted disease. *Circulation.* 2008;117:2938–2948.
16. Lamprea-Montealegre JA, McClelland RL, Astor BC, et al. Chronic kidney disease, plasma lipoproteins, and coronary artery calcium incidence: the Multi-Ethnic Study of Atherosclerosis. *Arterioscler Thromb Vasc Biol.* 2013;33:652–658.
17. Sage AP, Tintut Y, Demer LL. Regulatory mechanisms in vascular calcification. *Nat Rev Cardiol.* 2010;7:528–536.
18. Segall G, Delbeke D, Stabin MG, et al. SNM practice guideline for sodium ^{18}F-fluoride PET/CT bone scans 1.0. *J Nucl Med.* 2010;51:1813–1820.
19. Boellaard R, Delgado-Bolton R, Oyen WJ, et al. FDG PET/CT: EANM procedure guidelines for tumour imaging—version 2.0. *Eur J Nucl Med Mol Imaging.* 2015;42:328–354.